Numerical investigation of the effect of motion trajectory on the vortex shedding process behind a flapping airfoil

Ali Boudis, Annie-Claude Bayeul-Lainé, Ahmed Benzaoui, Hamid Oualli, Ouahiba Guerri

Numerical investigation of the effect of motion trajectory on the vortex shedding process behind a flapping airfoil

Ali Boudis [1,4], Annie-Claude Bayeul-Lainé[2]*, Ahmed Benzaoui[1], Hamid Oualli[3] , Ouahiba Guerri[4]

ISROMAC 2017

International Symposium on Transport Phenomena and Dynamics of Rotating Machinery

Maui, Hawaii

December 16-21, 2017

Abstract

The effect of non-sinusoidal trajectory on the propulsive performances and the vortex shedding process behind a flapping airfoil is investigated in this sutdy. A movement of a rigid NACA 0012 airfoil undergoing a combined heaving and pitching motions at low Reynolds number (11 000) is considered. An elliptic function with an adjustable parameter S (flatness coefficient) is used to realize various non-sinusoidal trajectories. The two-dimensional unsteady and incompressible Navier-Stokes equation governing the flow over the flapping airfoil is resolved using the commercial software STAR CCM+. It is shown that the combination of sinusoidal and non-sinusoidal flapping motion has a great effect on the propulsive performances of the flapping airfoil. The maximum propulsive efficiency is always achievable with sinusoidal trajectories. However, non-sinusoidal trajectories are found to considerably improuvr the propulsive force up to 52% larger than its natural value. Flow visualization shows that the vortex shedding process and the wake structure are substantially altered under the non-sinusoidal trajectory effect. Depending on the nature of the flapping trajectory, several modes of vortex shedding are identified and presented in this paper.

Keywords

Flapping airfoil — Aerodynamics — Non-sinusoidal trajectory — CFD

[1] *Laboratory of Thermodynamics and Energy Systems, Faculty of Physics, USTHB , BP 32 El-Alia Bab Ezzouar, Algiers, Algeria*

[2] *LMFL, FRE CNRS 3723, Arts et Metiers PARISTECH 8, Boulevard Louis XIV 59000 Lille, France*

[3] *Ecole Militaire Polytechnique, Laboratoire de Mécanique des Fluides, Algiers, Algeria*

[4] *Centre de Développement des Energies Renouvelables, CDER, BP 62 Route de l'Observatoire, Bouzaréah, 16340, Alger, Algérie*

*__Corresponding author__: Annie-Claude.BAYEUL-LAINE@ensam.eu

INTRODUCTION

In aeronautics, the field of micro air vehicle (MAV), and in particular micro air vehicle with flapping wing, is one of the most studied subjects in recent years. The remarkable interest in the study of these small aircrafts is linked to the advantages of this locomotion mode. Unlike the fixed-wing, flapping-wing MAV are able to perform hovering or low-speed flight in the manner of insects or humming birds with very high manoeuvrability. They perform punctual tasks,the flapping wings offer the advantage related to the acoustic spectrum generally lower than that created by the rotating wings. In addition, flapping wings MAV develop a higher lift force than that of the fixed and rotating wings due to non-stationary flow aspect. To generate the same lift force, the latter need more energy supply.

Historically, Knoller [1] and Betz [2] are among the pioneers to suggest a quasi-steady approach to explain the lift and thrust generation mechanism using a flapping wing. The Knoller-Betz effect stipulate that during a flapping motion, wings create an unsteady effective Angle of Attack (AoA) due to the transversal velocity, giving birth consequently an aerodynamic force with both lift and thrust components. In 1922, Katzmayr [3] carried out the first experimental work to verify Knoller-Betz effect and to confirm the possibility of thrust production using flapping wings. Thereafter, von Karman and Burgers [4] provide the relationship between the wake nature and the drag or thrust production. A drag-indicative wake (Fig. 1-a), similar to the von Karman eddy street observed behind a bluff body is formed when the lower vortex row is counterclockwise and the upper clockwise. The reverse von Karman vortex street (Fig. 1-b) with clockwise upper vortex and counterclockwise lower vortex is a thrust-indicative wake. A year later, Theodorsen [5] successfully calculated the unsteady forces and moments generated by an airfoil in harmonic motion using the hypothesis of incompressible potential flow with the Kutta condition at the trailing edge. Subsequently, Garrick [6] continued the work of Theodorsen [5] where he theoretically showed that an airfoil in pure heaving motion generates thrust for all frequencies, while pure pitching airfoil generates thrust above a certain critical frequency.

Since the first explanation of thrust generation from flapping airfoil, several experimental ([7], [8], [9], [10], [11],[12], [13], [14]) and numerical studies ([15], [16], [17], [18], [19], [20], [21], [22]) are performed on flow over flapping airfoil to understand the mechanism of thrust generation and improve their propulsive performances. Presently, research are oriented towards better energy saving and efficiency by increasing aerodynamic performances of micro air vehicle with adequate technological solutions. In this context, it is endeav-

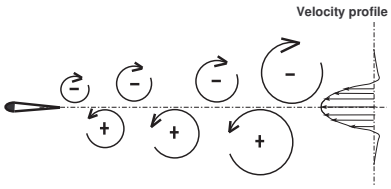

(a) Drag-indicative wake

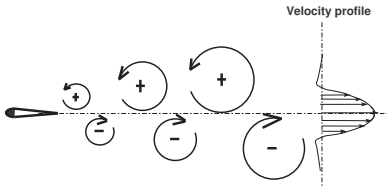

(b) Thrust-indicative wake

Figure 1. Vortical patterns in the wake of a flapping airfoil.

oured here to study the effect of the trajectory motion on the propulsive performances and the vortex shedding mechnism of a flapping airfoil. To this aim, the commercial code STAR CCM+ is used to solve the unsteady laminar flow over an airfoil executing a flapping movement reproduced using the overset mesh technique available in the environment. Reliability and accuracy of the numerical procedure is examined by comparing the computed results with experimental and numerical literature results ([9],[18]).

1. NUMERICAL MODELISATION

1.1 Flapping motion kinematics

The sinusoidal flapping motion of an airfoil (Fig.2) is given by the following equations:

$$h(t) = h_0 c \cos(\omega.t) \tag{1}$$

$$\theta(t) = \theta_0 \cos(\omega.t + \phi) \tag{2}$$

Where $h(t)$ and $\theta(t)$ are the heaving and the pitching motions respectively, h_0 is the heaving amplitude, θ_0 the pitching amplitude, $\omega = 2\pi f$ is the angular frequency, c is the chord length and ϕ is the angle phase between the heaving and the pitching motions. The pitch axis is located at 1/3 of the chord from leading edge.

The non-sinusoidal flapping motion is realized using an elliptical trajectory defined by the following equation:

$$F(t) = \frac{S\cos(\omega.t)}{\sqrt{S^2\cos(\omega.t)^2 + \sin(\omega.t)^2}} \tag{3}$$

Where S is an adjustable parameter. As shown in Fig. 3, when $S = 1$ the elliptical trajectory is sinusoidal. if S tends to infinity a square trajectory is obtained.

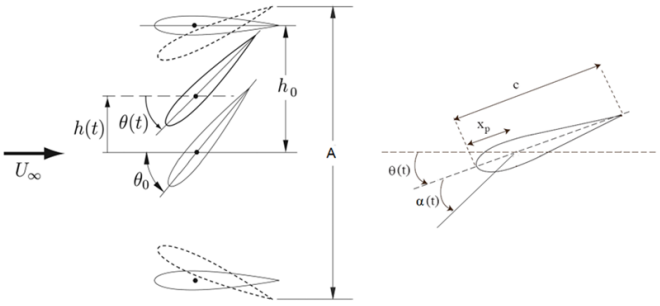

Figure 2. Main kinematic parameters of a flapping airfoil .

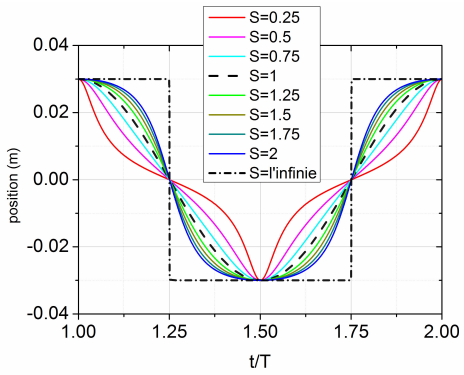

Figure 3. Flapping trajectories according to different values of the adjustable parameter S.

In the case of a non sinusoidal trajectory, the combined heaving and pitching motions can be represented by:

$$h_0(t) = h_0 c \frac{S_h \cos(\omega.t)}{\sqrt{{S_h}^2\cos(\omega.t)^2 + \sin(\omega.t)^2}} \tag{4}$$

$$\theta(t) = \theta_0 \frac{S_\theta \cos(\omega.t + \phi)}{\sqrt{{S_\theta}^2\cos(\omega.t + \phi)^2 + \sin(\omega.t + \phi)^2}} \tag{5}$$

Where S_h and S_θ are the adjustable parameters of heaving and pitching trajectory respectively.

When the airfoil is moving, the effective angle of attack $\alpha(t)$ is the sum of the pitching angle and the induced angle due to plunging motion. This angle is given by the relation:

$$\alpha(t) = \arctan(\frac{1}{U_\infty}\frac{dh(t)}{dt}) - \theta(t) \tag{6}$$

In addition, two dimensionless parameters are used to characterize the propulsive performance of the flapping airfoil. The Strouhal number defined by Anderson [9] as $St = 2cfh_0/U_\infty$ and the Reynolds number based on the chord length of the airfoil, $Re = \rho c U_\infty/\mu$, where ρ is the flow density , U_∞ is the free-stream velocity and μ is the dynamic viscosity.

1.2 Thrust and propulsive efficiency definition

The propulsive performance of a flapping airfoil can be quantified by calculating the mean thrust coefficient $\bar{C}_t$, the mean

power coefficient $\bar{C_p}$ and the propulsive efficiency η.

$$\bar{C_t} = -\frac{1}{T}\int_0^T C_D(t)dt \tag{7}$$

$$\bar{C_p} = -\frac{1}{T}\int_0^T (\frac{1}{U_\infty}C_L(t)\frac{dh(t)}{dt} + \frac{c}{U_\infty}C_Z(t)\frac{d\theta(t)}{dt})dt \tag{8}$$

$$\eta = \frac{\bar{C_t}}{\bar{C_p}} \tag{9}$$

Where T is the period of motion. C_D ,C_L and C_Z are respectively the drag, lift and moment coefficients, defined as follows :

$$C_D = \frac{F_x}{0.5\rho A{U_\infty}^2},\ C_L = \frac{F_y}{0.5\rho A{U_\infty}^2},\ C_Z = \frac{M_z}{0.5\rho cA{U_\infty}^2}$$

Where A is the area of the airfoil. The pitching axis is located at 1/3 of the chord length from the leading edge.

1.3 Navier-Stokes Solver

The numerical simulations are performed using the finite volume code STAR-CCM+. A segregated pressure based solver was used to solve the Navier-Stokes equations with a pressure-velocity coupling achieved by the Semi-Implicit Method for Pressure-Linked Equations (SIMPLE). The Second Order schemes are used for the pressure and momentum discretization and the unsteady formulation is based on a second-order implicit scheme. The flow is considered to be laminar and incompressible in all the simulations.

1.4 Computational domain and boundaries conditions

The dimensions of the computational domain and the boundary conditions used in this study are schematically shown in Fig. 4. The domain is subdivided into two zones: a background zone and an overset zone. The airfoil is located in the zone 1 (overset zone). This zone is moving to ensure the heaving and pitching motions. It is meshed with a very fine structured mesh to accurately capture the gradients in the area close to the airfoil surface. As in [19] the first grid point is located at $10^{-5}c$ giving $y+$ less than 1. The second zone (Background) is also meshed with a structured mesh but less dense compared with the first zone to decrease the cells number and improve the calculation efficiency. The connection between the two zones is ensured using the overset mesh interface [23]. The overset mesh technique allows to simulate the combined heaving and pitching motions without using other techniques such as deforming mesh or re-meshing.

In this study, the considered mesh consists of 304569 cells and the time step is defined as $\delta t = T/1000$. The mesh and the time step are chosen on the basis of a sensitivity study which is not presented here.

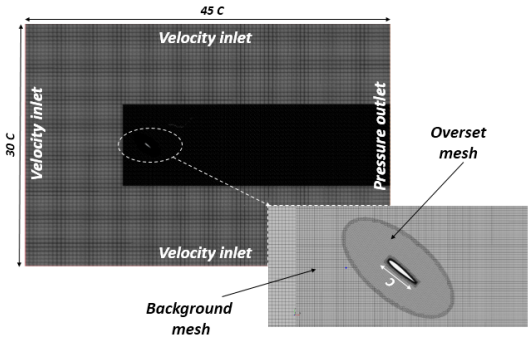

Figure 4. Computational domain and boundary conditions.

1.5 Validation

To confirm the accuracy of the present approach, the computed results were compared with the experimental and numerical results available in the literature. The propulsive performance of a $NACA0012$ airfoil undergoing a combined heaving and pitching motions at low Reynolds number (Re = 40 000) are calculated using the following kinematic parameters $h_0 = 0.75$, $\alpha_0 = 15°$ and $\phi = 90°$ and a Strouhal number St_{TE} varying in the range $[0, 0.5]$, ($St_{TE} = fA_{TE}/U_\infty$, where A_{TE} is the maximum excursion of the trailing edge [9]). The obtained results, in terms of thrust coefficient, power coefficient, and the propulsive efficiency, Fig. 5, are compared to those achieved experimentally by [9] and to numerical results obtained by [18] and our own results obtained using Fluent [24]. Our results underestimates the experimental data but are in good agreement with the numerical results.

2. RESULTS AND DISCUSSION

The wake structure downstream of the trailing edge plays a significant role on the forces generated by a flapping airfoil [25]. In this context, the present study is carried out to evaluate and quantify the effects of non-sinusoidal flapping trajectory on the propulsive performance and on the vortex formation, shedding process and the wake pattern behind a flapping airfoil. To carry out this study three cases are considered:

- Case 1: Non-sinusoidal heaving combined with sinusoidal pitching motions.
- Case 2: Sinusoidal heaving combined with non-sinusoidal pitching motions.
- Case 3: Non-sinusoidal heaving and pitching motions.

To study the effect of motion trajectory, the kinetics parameters are fixed as: $h_0 = 0.3$, $\phi = 90°$,$\alpha_0 = 15°$, $St \in [0.1 - 0.5]$ and $Re = 11\,000$. The non-sinusoidal trajectory are obtained by modifiying the flattening coefficient in the range of $[0.25 - 2]$. The obtained results are compared to those of a sinusoidal trajectory case to show the influence of the nature of motion trajectory on the airfoil propulsive performance. The table **??** summarizes the studied cases.

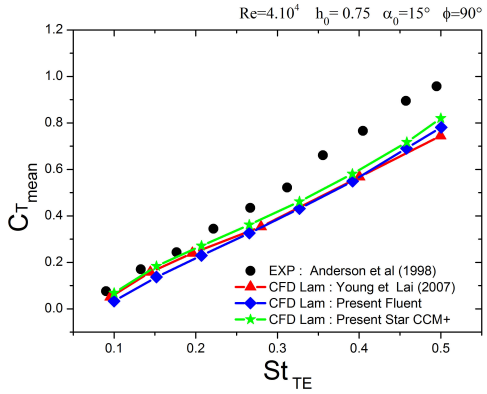

(a) Mean thrust coefficient

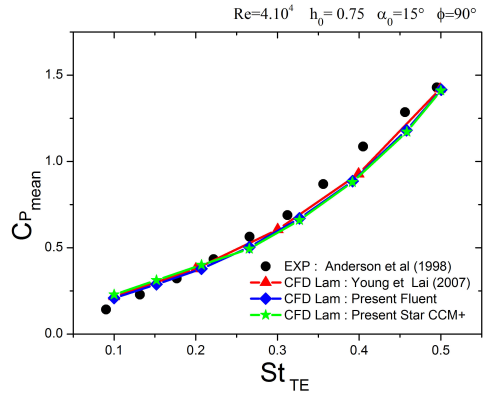

(b) Mean input power coefficient

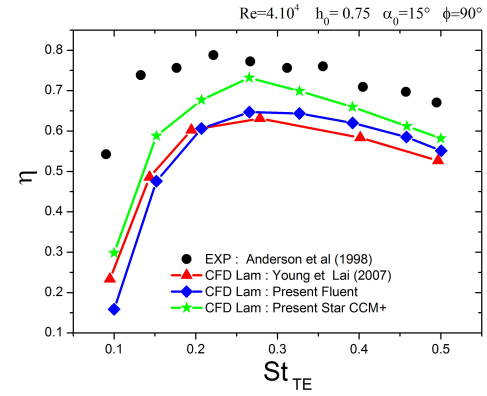

(c) Propulsive efficiency

Figure 5. Variation of $\bar{C_t}$, $\bar{C_p}$ and η with St_{TE}.

Table 1. Case analyzed

	Flattering coefficient S	
	Heaving traj S h	Pitching traj S theta
Referance case (Sinusoidal trajectory)	1	1
Case 1	0.25	1
	0.5	
	1.5	
	2	
Case 2	1	0.25
		0.5
		1
		2
Case 3	0.25	0.25
	0.5	0.5
	1	1
	2	2

2.1 Effect of Strouhal number

In this section, the effect of Strouhal number on the performance of the flapping airfoil is investigated. The variation of the mean thrust coefficient($\bar{C_t}$), mean power coefficient ($\bar{C_p}$) and the propulsive efficiency η with St for different values of S_h and S_θ are shown in (Fig. 6, 7 and 8). In the three cases, it is observed that the increase in the Strouhal number induces an increase of the mean thrust coefficient and the mean power coefficient . This is in good agreement with the experimental results of [9]. These authors mentioned that the mean coefficient of thrust increases continuously with the increase of the Strouhal number. It is also observed that the propulsive efficiency increases with the increase of the Strouhal number up to a threshold value $St = 0.2$ and then decreases. This decreasing tendency is due to the fact that, at high Strouhal numbers, the power consumed increases more rapidly to maintain the flapping motion.

2.2 Effect of non-sinusoidal trajectory

The effect of the non-sinusoidal trajectory on the propulsive performances of the flapping airfoil assessed for a fixed Strouhal number ($St = 0.2$, case of the best propulsive efficiency). The obtained results are presented in Fig. 9. It is seen that the propulsive efficiency obtained with sinusoidal trajectory is always better than that obtained by the non-sinusoidal trajectory regardless the the value of flattening coefficient. On the other hand, the thrust force obtained with non-sinusoidal trajectories is notably improved compared to the sinusoidal trajectories. In the case of a non-sinusoidal heaving, it is observed that the best propulsive force is achieved with the trajectories corresponding to the flattening coefficient values larger than 1. However, in the case of non-sinusoidal pitching, the best propulsive force is obtained with the trajectories realized by the use of flattening coefficient less than 1. For this case, the power consumed to maintain the flapping motion is weak compared to the other

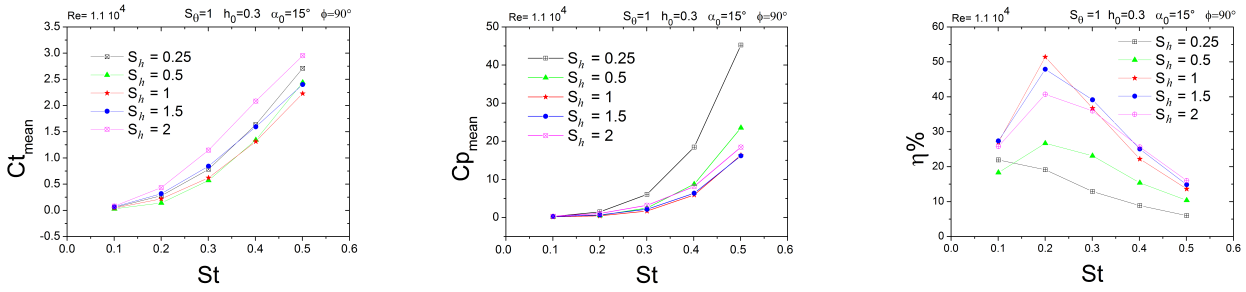

(a) Mean thrust coefficient (b) Mean input power coefficient (c) Propulsive efficiency

Figure 6. Effect of non-sinusoidal heaving, Case 1.

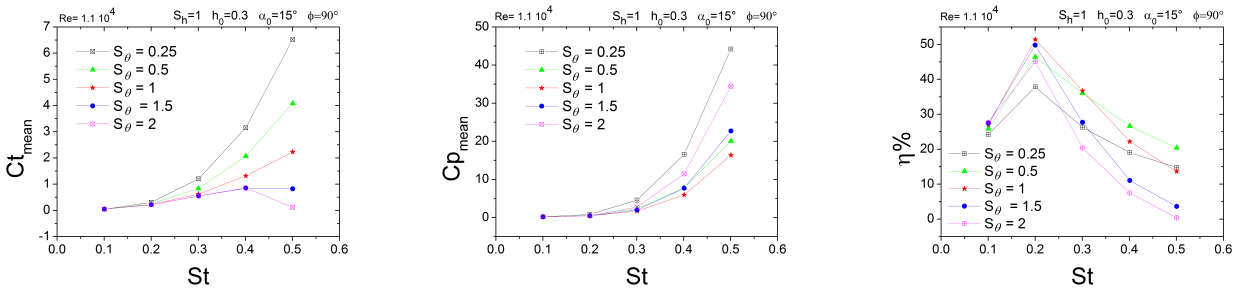

(a) Mean thrust coefficient (b) Mean input power coefficient (c) Propulsive efficiency

Figure 7. Effect of non-sinusoidal pitching, Case 2.

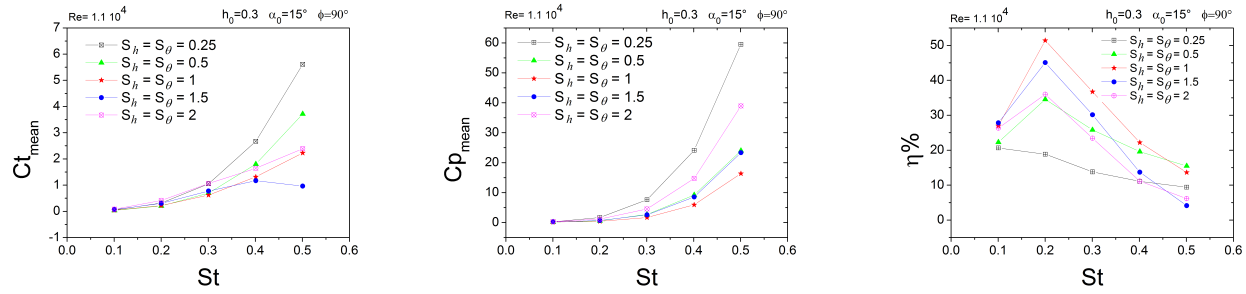

(a) Mean thrust coefficient (b) Mean input power coefficient (c) Propulsive efficiency

Figure 8. Effect of non-sinusoidal heaving and pitching motions, Case 3.

cases. This results in a better propulsive efficiency whatever is the value of the flattening coefficient. For all the considered situations, it is found that using trajectories realized with the use of flattening coefficients less than 1 requires more energy to maintain the flapping motion. It is found also that heaving trajectory has significant effect on propulsive performances of flapping airfoil compared to the pitching trajectory. This is mainly due to the kinematic angle of attack induced by the heaving motion(see Fig. 10).

To better understand how the motion trajectory affects the flapping airfoil propulsive performances, we have made some quantitative comparisons relative to the instantaneous aerodynamic coefficients (CD and CL) and some qualitative comparisons by visualizing the wake structure behind the flapping airfoil.

2.2.1 Effect on the aerodynamic coefficients

The non-sinusoidal heaving and pitching motions modified deeply the flow structure and the vortex shedding process behind the flapping airfoil. this substantially impacts on the drag (CD) and lift (CL) coefficients. Figure 11 shows time variation of the CD and CL over one flapping cycle. A remarkable behavior of the drag and lift coefficients is observed when compared to the reference case (sinusoidal trajectory) where CD and CL adopt a pseudo-sinusoidal shape. In all cases, the drag coefficients are practically negative, indicative of thrust production. Moreover, high values of negative drag coefficients are obtained by the non-sinusoidal trajectories

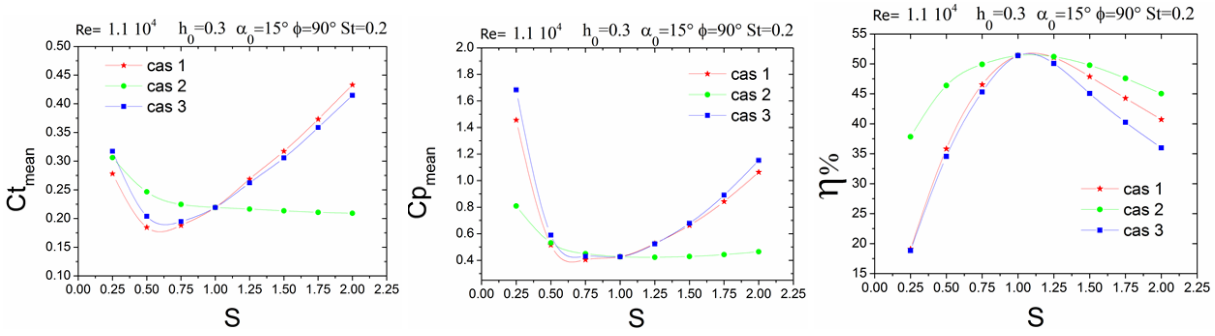

(a) Mean thrust coefficient (b) Mean input power coefficient (c) Propulsive efficiency

Figure 9. Effect of the flapping trajectory on the propulsion performances.

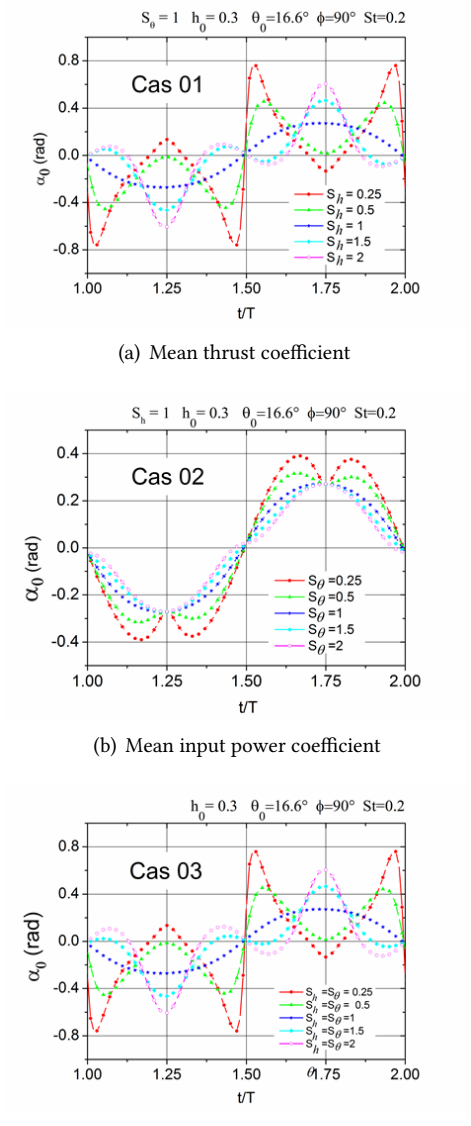

(a) Mean thrust coefficient

(b) Mean input power coefficient

(c) Propulsive efficiency

Figure 10. Effect of the flapping trajectory on the kinematic angle of attack.

corresponding to the flattening coefficients greater than 1. The best lift coefficients are registered for non-sinusoidal trajectories realized by the use of flattening coefficients less than 1.

In conclusion, if a better propulsive force are sought, it is advantageous to use non-sinusoidal trajectories realized by flattening coefficients greater than 1. However, if a better lift force are searched, it is advisable to use non-sinusoidal trajectories realized by flattening coefficients less than 1 are recommended.

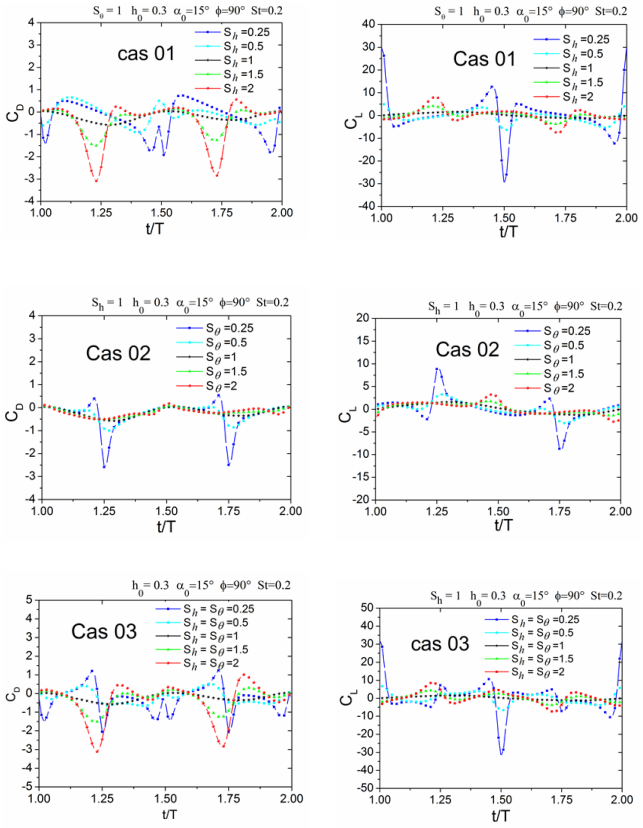

Figure 11. Time variation of CD and CL under the effect of non-sinusoidal motion.

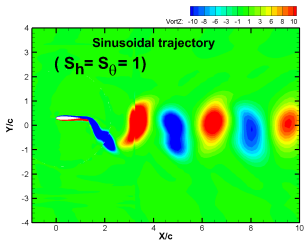

Figure 12. The $2S$ vortex shedding mode.

2.2.2 *Effect on the vortex shedding process*

The flow visualization around the flapping airfoil shows that the vortex shedding process is greatly affected by non-sinusoidal trajectory. In fact, the wake rearranges in new configurations different to that of the sinusoidal case.

The symbols S and P introduced by Williamson and Roshko in 1988 [26] to classify the vortex shedding modes are adopted.

Reference Case (Sinusoidal flapping motion): The $2S$ mode (Fig. 12) is observed in the reference case (Sinusoidal flapping motion, $S_h = S_\theta = 1$). In this mode, two vortices are shed per cycle.

the first one, shed in the upstrok phase is clockwisely rotating while the second one, produced during the down-stroke phase, is counter-clockwisely rotating. Tis vortices pair travels along the wake medium line. The interaction between these vortices produce a je-like flow directed downstream of the trailing edge which, by reaction, generates a thrust force directed upstream. In this work, the $2S$ mode is associated with the case of the best propulsive efficiency.

Case of non-sinusoidal flapping motion : A combination between the sinusoidal and non-sinusoidal flapping motions shows new wake configurations ($2S$, $2P$, $2P_0$), as shown in Fig.13, 14 and 15 .

- ☐ The $2P$ vortex shedding mode : This mode appeared for both following cases: $S_h < 1$ and/or $S_\theta > 1$. In this mode, two counter-rotating vortices are shed in each half-cycle, the first vortex is formed on the leading edge (LEV) and the second is formed on the trailing edge (TEV) releasing two vortices pair per cycle. In $2P$ mode, the vortex shedding frequency remains equal to the frequency of $2S$ mode [27]. The $2P$ vortex shedding mode causes a large increase in the lifting force compared to that given by the sinusoidal trajectory. This is explained by the intensity of the vortex formed at the leading edge.

- ☐ The $2P_0$ vortex shedding mode : The $2P_0$ mode is a transition mode between $2S$ and $2P$. This mode was identified by Morse and Williamson (2009) during their studies on the flow controlled by an oscillating cylinder. In the $2P_0$ mode, the airfoil shed two counter-rotating vortices in each half cycle, as in the $2P$ mode. However, in $2P_0$ mode, the first vortex has a high intensity compared to the second vortex which is much weaker and disappear rapidly in the wake. In this mode the far wake is similar to that of the $2S$ mode.

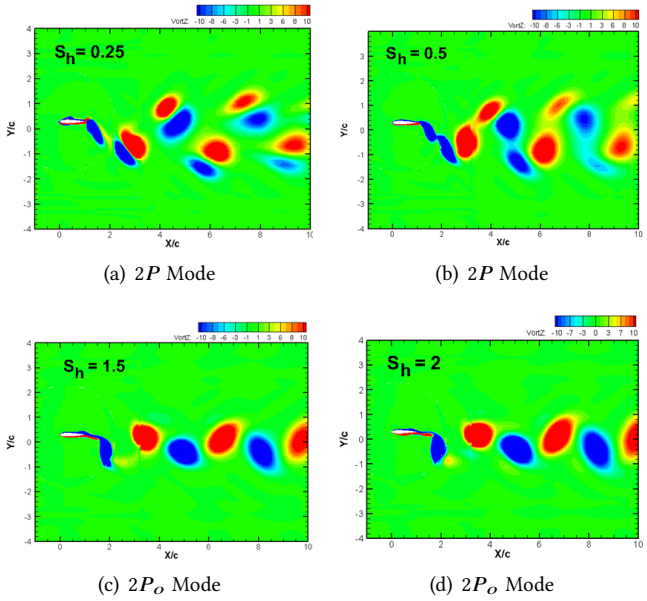

(a) $2P$ Mode (b) $2P$ Mode

(c) $2P_o$ Mode (d) $2P_o$ Mode

Figure 13. Modes of vortex shedding and the wake pattern, Case 1.

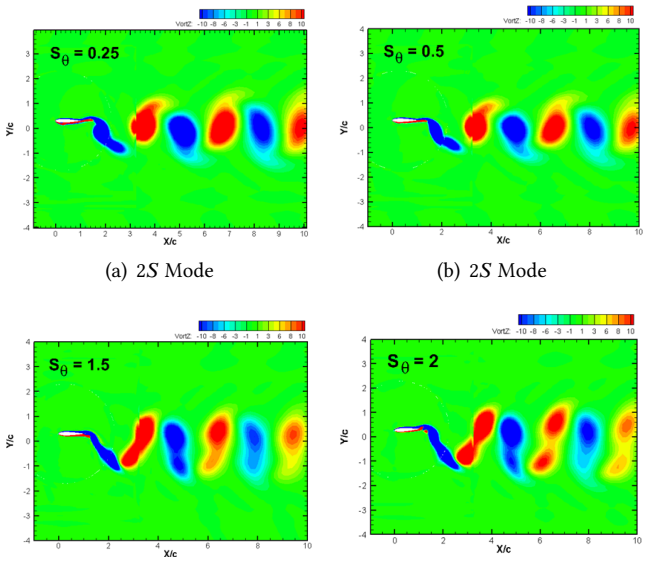

(a) $2S$ Mode (b) $2S$ Mode

(c) $2P$ Mode (d) $2P$ Mode

Figure 14. Modes of vortex shedding and the wake pattern, Case 2.

CONCLUSION

In this study, the effects of motion trajectory on the propulsive performances and the shedding process of a flapping airfoil are examined. The flow structures and the forces acting on NACA 0012 airfoil undergoing sinusoidal and non-

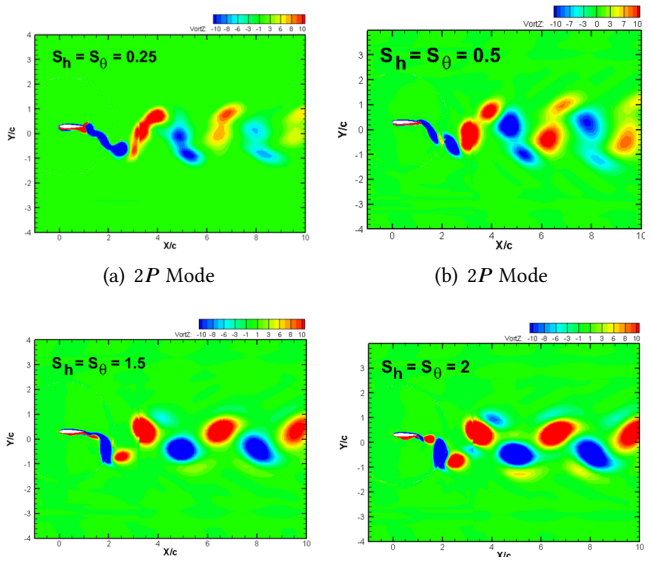

(a) $2P$ Mode (b) $2P$ Mode

(c) $2P_o$ Mode (d) $2P_o$ Mode

Figure 15. Modes of vortex shedding and the wake pattern, Case 3.

sinusoidal heaving and pitching motions are investigated using the finite volume code STAR CCM+. The results obtained in the validation step show the ability of our numerical investigation to reproduce physical phenomennology obtained by experimentation. It is established that the trajectory motion has a significant effect on the performances and the vortex-shedding mode of the flapping airfoil. The best propulsive efficiency is always obtained by the sinusoidal flapping trajectory. However, the use of non-sinusoidal flapping trajectory enhanced considerably the aerodynamic characteristics of the flapping airfoil in terms of the propulsive and the lifting forces. Qualitatively, it is observed that the vortex-shedding mode shifts from $2S$ a sinusoidal trajectory to other configurations ($2S$, $2P$, $2P_0$) for non-sinusoidal trajectory. Lai and Platzer [14] have concluded that the signature of the wake and the mode of vortex shedding mode behind a flapping airfoil depends on the Strouhal number. This is confirmed in this study. In addition to the Strouhal number, the nature of the flapping trajectory (sinusoidal and non-sinusoidal) affects considerably the propulsive performances as well as the vortex shedding mode of the flapping airfoil.

REFERENCES

[1] R. Knoller. Die gesetze des luftwiderstands. In *Flug und Motortechnik*, pages 1 – 7, German, 1909.

[2] R. Knoller. Zeitschriftfaurflugtechnik und motorluftschiffahrt. In *Einbeitragzurerklarung des segelfluges*, pages 269 – 272, German, 3 1912.

[3] R. Katzmayr. Effect of periodic changes of angle of attack on behaviour of airfoils. In *NACATM-147*, National Advisory Committee for Aeronautics; Washington, DC, United States, Oct 01 1922.

[4] T. Von Kármán and J. M. Burgers. Aerodynamic theory. *Springer*, 2, 1934.

[5] T. Theodorsen. General theory of aerodynamic instability and the mechanism of flutter. In *NASA Report*, number 496, 1922.

[6] I. E. Garrick. Propulsion of a flapping and oscillating airfoil. In *NACA Report*, number 567, 1937.

[7] M.M. Koochesfahani. Vortical patterns in the wake of an oscillating airfoil. *AIAA Journal*, 9(27):1200 – 1205, 1989.

[8] Triantafyllou M.S. A. G.M. Triantafyllou, G.S. Optimal thrust development in oscillating foils with application to fish propulsion. *Journal of Fluids and Structures*, 7:205 – 224, 1993.

[9] J. M. Anderson, K. Steritlien, D. S. Barrett, and M. S. Triantafyllou. Oscillating foils of high propulsive efficiency. *Journal of Fluid Mechanics*, 360:41–72, 1998.

[10] Platzer M.F. Lai, J.C.S. Jet characteristics of a plunging airfoil. *AIAA Journal*, 37(12):1529 – 1537, 1999.

[11] Hover F.S. Triantafyllou M.S. Read, D.A. Forces on oscillating foils for propulsion and maneuvering. *Journal of Fluids and Structures*, 17(1):163 – 183, 2003.

[12] Techet A.H. Hover F.S. Triantafyllou, M.S. Review of experimental work in biomimetic foils. *IEEE Journal of Oceanic Engineering*, 29(3):585 – 594, 2004.

[13] Tuan Anh Nguyen, Hoang Vu Phan, Thi Kim Loan Au, and Hoon Cheol Park. Experimental study on thrust and power of flapping-wing system based on rack-pinion mechanism. *Bioinspiration and Biomimetics*, 11(4):046001, 2016.

[14] M. N. P. Babu, P. Krishnankutty, and J. M. Mallikarjuna. Experimental study of flapping foil propulsion system for ships and underwater vehicles and piv study of caudal fin propulsors. In *2014 IEEE/OES Autonomous Underwater Vehicles (AUV)*, pages 1–7, Oct 2014.

[15] Platzer M.F. Tuncer, I.H. Thrust generation due to airfoil flapping. *AIAA Journal*, 34(2):324 – 331, 1996.

[16] Berg M. Ljungqvist D. Shyy, W. Flapping and flexible wings for biological and micro air vehicles. *Progress in Aerospace Sciences*, 35(5):455 – 505.

[17] Lai J.C.S. Young, J. Oscillation frequency and amplitude effects on the wake of plunging airfoil. *AIAA Journal*, 42(10):2042 – 2052, 2004.

[18] J. Young and J.C.S. Lai. Mechanisms influencing the efficiency of oscillating airfoil propulsion. *AIAA*, 45:1695 – 702, 2007.

[19] M. A. Ashraf, J. Young, J.C.S. Lai, and M.F. Platzer. Numerical analysis of an oscillating-wing wind and hydropower generator. *AIAA J*, 49(7):1374 – 1386, 2011.

[20] T. Benkherouf, M. Mekadem, H. Oualli, S. Hanchi, L. Keirsbulck, and L. Labraga. Efficiency of an auto-

propelled flapping airfoil. *Journal of Fluids and Structures*, 27(4):552 – 566, 2011.

[21] Mathieu Olivier and Guy Dumas. Effects of mass and chordwise flexibility on 2d self-propelled flapping wings. *Journal of Fluids and Structures*, 64:46 – 66, 2016.

[22] Li-Ming Chao, Yong-Hui Cao, and Guang Pan. A review of underwater bio-mimetic propulsion: cruise and fast-start. *Fluid Dynamics Research*, 49(4):044501, 2017.

[23] Star ccm+ user guide. url http://www.cd-adapco.com/products/star-ccm.

[24] A. BOUDIS, M. MEKADEM, H. OUALLI, A. BENZAOUI, and O. GUERRI. Etude numérique de l'influence des paramètres de mouvement sur les performances aérodynamiques d'une aile battante. In *2ème conference international sur l'énergétique appliquée et la pollution "CIEAP'14"*, Constantine, Algérie, 14-15 Décembre 2014.

[25] Qing Xiao and Wei Liao. Numerical investigation of angle of attack profile on propulsion performance of an oscillating foil. *Computers and Fluids*, 39(8):1366–1380, 9 2010.

[26] A. Williamson, C. H. K.; Roshko. Vortex formation in the wake of an oscillating cylinder. *Journal of Fluids and Structures*, 2:355 – 381, 1988.

[27] Williamson C. Govardhan, R. Modes of vortex formation and frequency response of a freely vibrating cylinder. *Journal of Fluid Mechanics*, 420:85 – 130, 2000.